

## DETERMINATION OF COMPARATIVE BIOLOGICAL ACTIVITIES OF SILVER NANOPARTICLES FORMED BY BIOLOGICAL SYNTHESIS USING *ACHILLEA VERMICULARIS*

BÜLENT KAYA<sup>1\*</sup>, EKREM DARENDELİOĞLU<sup>1</sup>, GÖKHAN DERVIŞOĞLU<sup>1</sup> AND MUSA TARTIK<sup>1</sup>

<sup>1</sup> Bingol University, Science and Art Faculty, Molecular Biology and Genetics Department, 12000, Turkey

\*Correspondence author's email: b\_kaya\_tr@yahoo.com

### Abstract

Several researchers examined the production of nano-particles for their potential commercial advantages. Hazardous manufacturing methods of synthesizing nano-particles chemically have directed the research towards biological systems in producing nano-particles. The present study would explore the anti-bacterial property, anti-oxidation and anticancer activities of silver nano-particles with *Achillea vermicularis* in water extracts under different two temperatures. Furthermore, this study would examine the consequences of silver nano-particles, which affect human health and PC3 cell lines. Silver nano-particles have enormous uses due to their beneficial properties. Silver nano-particles are used in medicinal, industrial, nutritional, cosmetic, detergent, and medical devices. The biologically synthesized Silver nanoparticles were performed with redox. AvAgNPs were also characterized by UV-visible spectroscopy, scanning electron microscopy (SEM), transmission electron microscopy (TEM), Fourier transform infrared spectroscopy (FTIR) and X-ray diffraction (XRD). The biologically synthesized AvAgNPs showed effective antibacterial activity against Gram negative (*Escherichia coli*) and Gram positive (*Listeria monocytogenes*, *Staphylococcus aureus*) bacteria and yeast (*Saccharomyces cerevisiae*). WST assay analysis indicated potential anticancer characteristics. Antioxidant activity of all AvAgNPs were determined by total phenolic, total flavonoid, DPPH reduction activity, metal chelating activity, hydrogen peroxide reduction activity tests. Results indicated that AvAgNPs had potential antioxidant activity. Nano-particles collected by green synthesis could be a major source in commercial fields, therefore, silver nano-particles with *Achillea vermicularis* could be a good approach. The results of the present study demonstrated the potential of green synthesis of silver nanoparticles in reducing toxicity while retaining their antibacterial activities and boosting antioxidant activity of the extract.

**Key words:** Nanotechnology, Silver nanoparticles, Nanotoxicological, *Achillea vermicularis*

### Introduction

Nanotechnology is a scientific field that developed as a result of nanotoxicological research and advances. Subsequent manufacturing of chemicals derived from nanoparticles (NPs) attracted research interest. However, expressed that manufacturing NPs is chemically hazardous for the environment, and therefore, eco-friendly biological systems should be applied as an alternative (Thakkar *et al.*, 2010). Some researchers explained that NPs can be accumulated in plants and later harvested by various methods, such as sintering and smelting (Makarov *et al.*, 2014). Green syntheses of NPs gas have been carried out using *Brassica juncea*, which produced 50 nm of Ag NPs (Harris *et al.*, 2008), *Madia sativa* (*M. sativa*), which produced 4 nm Au NPs, and *Iris pseudacorus*, which produced 2 nm semi-spherical Cu NPs (Manceau *et al.*, 2008; Roh *et al.*, 2009). The present research considered the utilization of plants to produce metal NPs and also analysed the properties and effects of Ag NPs collected from *Achillea vermicularis*.

When Ag NPs are administered in low concentrations, they are effective against several kinds of microbes. The permeability of cells is altered in the presence of Ag particles, which eventually leads to cell necrosis (Rai *et al.*, 2009). Gram-negative (*Escherichia coli*) and Gram-positive (*Staphylococcus aureus*) bacteria have been tested against Ag particles, and the anti-microbial effects of Ag NPs against bacterial strains have been demonstrated (Barani *et al.*, 2011). The growth of *Staphylococcus aureus*, *Escherichia coli*, and *Serratia marcescens* has been found to decrease when cultured

with Ag particles (Oves *et al.*, 2013); Ag NPs also decrease the growth (Martínez-Gutierrez *et al.*, 2012). Moreover, Ag NPs have an anti-microbial property, which destroys bacterial cells and prevents rapid human-cell damage, and thus increases the longevity and well-being of the cell (Collart *et al.*, 2006; Zook *et al.*, 2011). The NPs are responsible for disrupting cell-to-cell adhesions between bacterial cell-lines and supporting their autolysis and catabolism.

Some researcher demonstrated that Ag NPs exhibit anti-oxidative properties that are useful in the cosmetics and detergent industries (Abdel-Aziz *et al.*, 2014). Moreover, when plant extracts are mixed with Ag NPs, the plant-extract Ag NPs exhibit an elevated anti-oxidative ability compared to only plant extracts (Mohanty *et al.*, 2012). The bleaching of organic dyes by applying potassium peroxodisulphate is increased when Ag NPs are added to the dyes (Liu *et al.*, 2010). Ag NPs also exhibit greater oxidative ability compared to Au and Pt particles (Abou El-Nour *et al.*, 2010). It is demonstrated that NPs, such as metalloids, which are produced by varying plant species, are used extensively in many industrial, medical, and electronic technologies due to their anti-oxidant properties (Sintubin *et al.*, 2009). Moreover, the anti-microbial ability is responsible for improving the effectiveness of certain chemicals (Kim *et al.*, 2012).

Ag NPs are widely utilized in many medical, industrial, and research fields, such as bio-sensing, food, paints, cosmetics, clothing, electronics, and medical devices (Ahamed *et al.*, 2010). Owing to the extensive use of metal particles, ecologists are concerned about the eco-health and

safety hazards caused by these particles (Gopinath *et al.*, 2008). In humans, Ag particles can enter the parenchyma and epithelial cells in the lungs, gastrointestinal tract, respiratory tract, and dermis, and exhibit therapeutic effects (Chen *et al.*, 2008; Zhang *et al.*, 2011).

*Achillea* (Asteraceae) species are used by Turkish people for treating several diseases. They are used to treat wounds, diarrhoea, abdominal pains, and cardiac diseases (Baytop, 1999). Previous studies that focused on *Achillea vermicularis* evaluated its cytotoxic activity against MCF-7 and A-549 cell lines (Hamzeloo-Moghadam *et al.*, 2015; Naghibi *et al.*, 2014).

In this study, for the first time, we investigated the biosynthesis of Ag NPs via a single-step reduction of Ag ions using *Achillea vermicularis* water plant extracts under two different temperatures, and from the viewpoint of biological activity, we studied the anti-oxidant activity of these biosynthesized Ag NPs against pure water plant extracts.

## Materials and Methods

**Materials:** All chemicals and reagents were procured from Merck (Darmstadt, Germany) and prepared in HPLC grade. RPMI 1640 medium containing 10% foetal bovine serum (FBS) and 1% penicillin-streptomycin solution was purchased from Biological Industries (Israel).

### Preparation of *Achillea vermicularis* flower extracts:

The extractions were prepared from flowers of *Achillea vermicularis*, which were previously washed several times with distilled water to remove the dust particles and then vacuum oven dried to remove the residual moisture. The dried flowers were powdered, and then, the plant material (20 g) was successively extracted by boiling in 250-ml glass beakers along with 200 ml of sterile distilled water for 30 min. As the solution came to the boiling point, the colour of the aqueous solution changed from transparent to yellow. The aqueous extract was separated by filtration with Whatman No. 1 filter paper and then centrifuged at 2000 rpm for 8 min to remove heavy biomaterials. *Achillea vermicularis* flower extracts were stored at  $-20^{\circ}\text{C}$  for the biosynthesis of Ag NPs from  $\text{AgNO}_3$  (Kaya *et al.*, 2012).

**Synthesis of AgNPs (AvAgNPs):** In a conventional reaction procedure for the flower, 5 ml of extract was added to 95 ml of  $1 \times 10^{-3}$  M aqueous  $\text{AgNO}_3$  solution to prepare two of the same mixtures from each extract, under magnetic stirring at  $40^{\circ}\text{C}$  and at room temperature. Two flower extract samples (F40 and F24) were used at  $40^{\circ}\text{C}$  and under room temperature ( $24^{\circ}\text{C}$ ). The yellow colour of the  $\text{AgNO}_3$  mixture and *Achillea vermicularis* flower extracts at 0 min of reaction time changed to a dark brown coloured mixture earlier (after 30 min) at  $40^{\circ}\text{C}$  when compared to the change under room temperature, which occurred after 1 h. After the colour change, samples were measured at 430 nm using a spectrophotometer to observe the formation of Ag NPs. AvAgNPs obtained by *Achillea vermicularis* F24 and F40 were centrifuged at 20,000 rpm for 10 min and subsequently dispersed in a pure water solution to get rid of any uncoordinated biological material (Awwad *et al.*, 2013).

**Characterization of AvAgNPs:** UV-vis spectrophotometer (Shimadzu UV-3600 UV-VIS-NIR Spectrophotometer) was used to determine the absorption spectra of the Ag NP samples within the scanning range of 200–900 nm using a 3–5 mm quartz cuvette. The pure water solution AvAgNPs were preferred as the blank.

The AvAgNPs were concentrated on glass surfaces using dry air for atomic force microscopy (AFM) characterization (Nanotechnology Park System NX 20) of the detailed size and morphology. Various magnifications were preferred for observation and were documented to view all sides of the sample.

The dimensional analysis of the produced AvAgNPs was conducted with zeta potential analysis ZETA Sizers Nanoseries (Malvern Instruments Nano ZS) to detect the size range. This instrument allows measurement of the distribution range and zeta potential of the particles.

Fourier transform infrared (FT-IR) spectra were measured by the dried pellet method in the  $4,000$  to  $400$   $\text{cm}^{-1}$  range (Perkin Elmer Spectrum 100) for the flower extract powders and the dried AvAgNPs. The FTIR analysis helped determine the functional groups and their possible involvement in the synthesis of AvAgNPs.

X-ray diffraction characterization of the dried AvAgNPs powder was carried out using a Rigaku Optima IV diffractometer with  $\text{Cu K}\alpha$  radiation ( $\lambda = 0.1542$  nm).

The morphology of the AvAgNPs was determined by scanning electron microscopy (SEM; JEOL). Before the analysis, the samples were 0.5% (w/v) doped with phosphotungstic acid, and placed on copper grids for investigation.

### Determination of total phenolic and flavonoid contents:

The total phenol amount in the extracts and AvAgNPs was determined using the Folin-Ciocalteu method (Gamez-Meza *et al.*, 1999). The total phenol amount in the samples was calculated from the calibration curve plotted with gallic acid, where it would equal to the gallic acid per mg.

The total flavonoid amount was determined based on previously prepared (+)-catechin standard calibration graph as a (+)-catechin match (Barros *et al.*, 2007).

**In vitro anti-oxidant assays:** DPPH radical scavenging assays for *Achiella vermicularis* and AvAgNPs were performed as described by Hatano *et al.* (1998). The DPPH radical removal activity was calculated using the formula below:

$$\% \text{ Inhibition} = (1 - A_{\text{Sample}}/A_{\text{Control}}) \times 100$$

where  $A_{\text{control}}$  is the absorbance of the control or the blind, and  $A_{\text{sample}}$  is the absorbance measured in the presence of the extract (Hatano *et al.*, 1988).

The metal chelating activity was analysed via the iron chelation property. The iron chelating activity of the extract was calculated using the formula below (Dinis *et al.*, 1994):

$$\text{Chelating Activity} = (1 - A_{\text{Sample}}/A_{\text{Control}}) \times 100$$

where  $A_{\text{control}}$  is the absorbance of the control or the blind, and  $A_{\text{sample}}$  is the absorbance measured in the presence of the extract.

The hydrogen peroxide removal activities of the AvAgNPs and water plant extracts were assayed using previously reported method. The H<sub>2</sub>O<sub>2</sub> removal activity was calculated using the following formula:

$$\text{H}_2\text{O}_2 \text{ Removal Activity} = (1 - A_{\text{Sample}}/A_{\text{Control}}) \times 100$$

where A<sub>Control</sub> is the absorbance of the control or the blind, and A<sub>Sample</sub> is the absorbance measured in the presence of the extract (Ruch *et al.*, 1989).

### Anti-microbial activity test

**Test microorganisms:** The green synthesized Ag NPs were tested for their anti-microbial activity against *Saccharomyces cerevisiae*, *Staphylococcus aureus*, *Listeria monocytogenes*, and *Escherichia coli*.

**Spread agar plate method:** The anti-microbial activity was tested using the spread plate agar method, in which 6 mm discs of the samples were placed on plates based on the number of trial agents. Using a micropipette, 30  $\mu$ l each of the AvAgNPs sample (1 mg/ml) and other agents were absorbed into the disks on all plates. During this test, a negative control (sterile pure water), a positive control (penicillin-streptomycin), the AvAgNPs, *Achillea vermicularis* flower extract, and flower extract + AgNO<sub>3</sub> were tested. After incubation at 34°C for 24 h, the diameter of the inhibition zone was measured.

**Cell culture:** Human prostate cells (PC-3) were used in the present study. Cells were procured from the American Type Culture Collection (ATCC, USA). The cells were cultured in an RPMI 1640 medium (Biological Industries, Israel) containing 10% FBS and 1% penicillin-streptomycin solution (Biological Industries, Israel). The cells were grown at 37 °C in a humidified incubator with 5% CO<sub>2</sub>, and sub-cultured every two or three days.

**Cell proliferation assay:** A WST-1 cell proliferation assay kit (Clontech, USA) was used to analyse cell

proliferation and viability. Cells were grown in T-25 flasks and harvested. Cells were counted using a Thoma hemocytometer. 5  $\times$  10<sup>3</sup> cells/well in a 100- $\mu$ l medium were seeded in a 96-well plate. After 24 h, various concentrations of *A. vermicularis* and AvAgNPs extracts were added to the wells in the 100- $\mu$ l medium. Cells were treated with 15,625–250  $\mu$ g/ml extract concentrations. After 48 h, 5  $\mu$ l of the WST-1 reagent was added to each well, and after 4 h of incubation, the absorbance was measured at 450 nm by using a SpectraMax Plus 384 microplate reader (Molecular Devices, USA). The reference absorbance was taken as 630 nm.

**Statistical analyses:** All measurements were repeated three times, and statistical analysis was performed with GraphPad Prism 5.01 software and comparable data sets were evaluated and the analyses were conducted using by one-way ANOVA (Analysis of variance) by Tukey's multiple comparison test and one-way ANOVA Newman-Keuls Post-Hoc Test with; p<0.05 was considered significant.

### Results and discussion

**Characterization of Ag NPs:** The researchers discovered a wide spectrum of surface plasmon resonance of Ag NPs and identified them at 430 nm (Kelly *et al.*, 2003). The colour of the AgNO<sub>3</sub> solution changed from transparent to yellow-brown with the addition of the *Achillea vermicularis* flower extract, indicating the start of NP formation. This colour change was due to the change in the Ag surface plasmon resonance. The UV-VIS\_NIR of Ag NPs formed a peak centred at 430 nm. (Fig. 1A, B). This showed that Ag ions were reduced to Ag NPs. NP and Ag ion reduction was completed in almost 2 h at room temperature (Veerasingam *et al.*, 2011).

The AFM images clearly show the surface morphology of AvAgNPs (Figs. 2A, B). In the 3D AFM image shown in Fig. 2C, D, spherical NPs can be observed. This particle morphology could be due to the AFM analysis sample preparation process (Jayaseelan *et al.*, 2013).

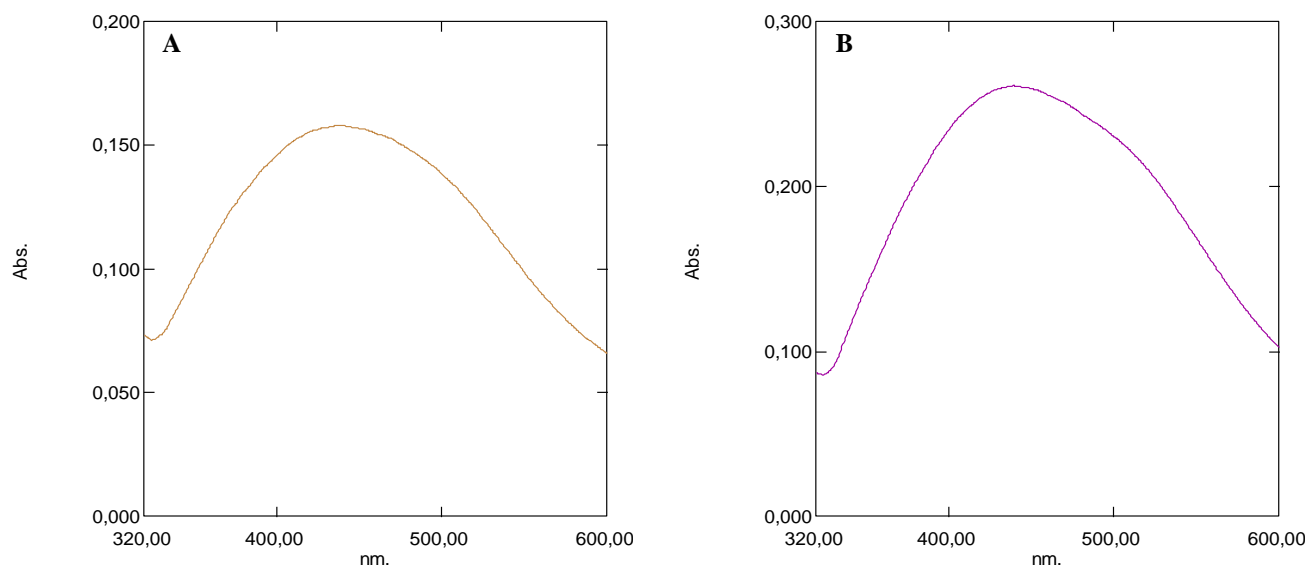


Fig. 1. UV-Vis absorption spectra of synthesized silver nanoparticles (A) AvAgNPs (Flower 24) (B). AvAgNPs (Flower 40).

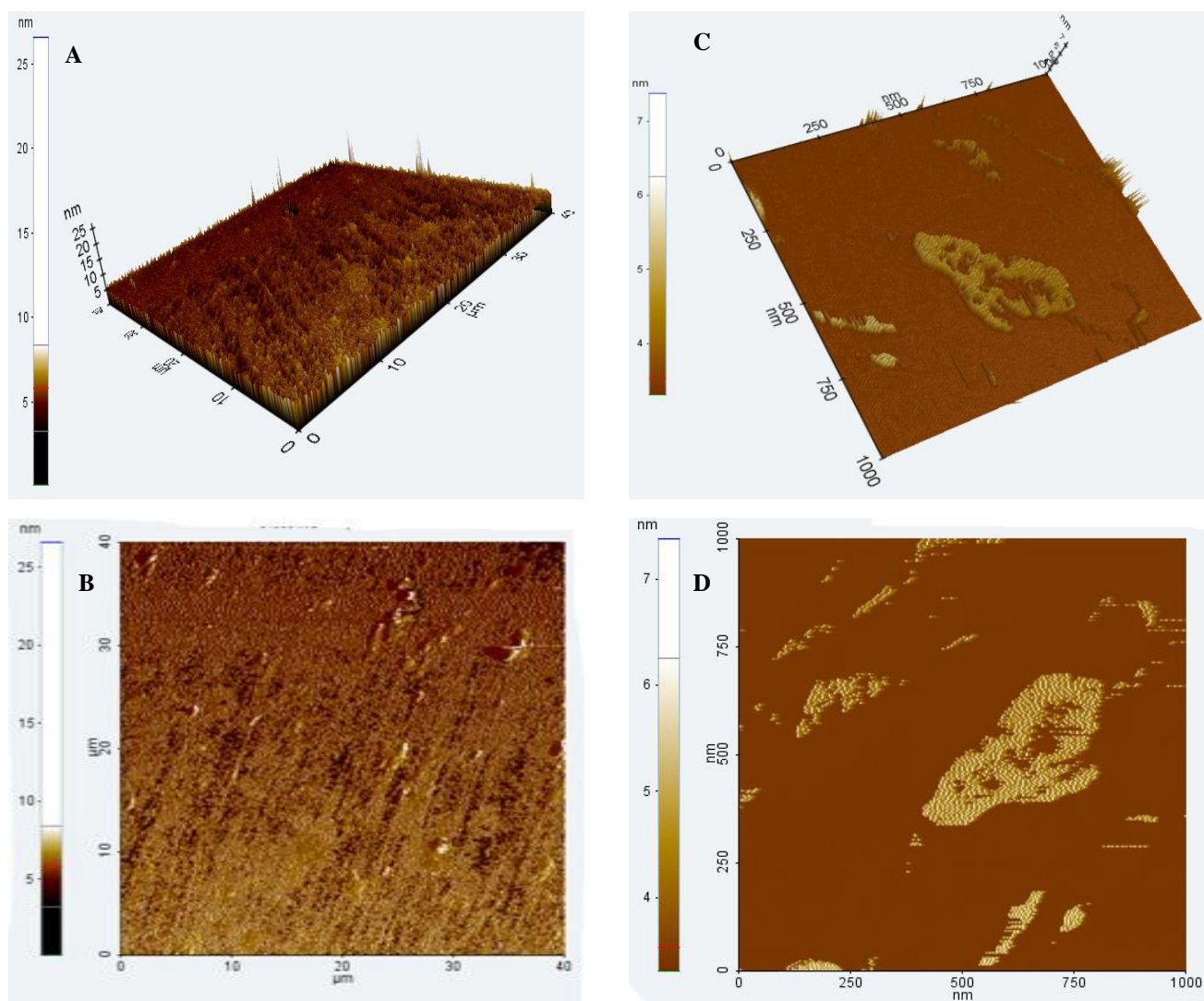


Fig. 2. AFM of synthesized silver nanoparticles (A) AvAgNPs 3D (Flower 24) (B). AvAgNPs (Flower 24) (C) AvAgNPs 3D (Flower 40) (D). AvAgNPs (Flower 40).

The zeta potential and particle size of the Ag NPs were also investigated (Figs. 3A and C). Under natural conditions (pH close to 7), the zeta potential of AvAgNPs F24 and F40 was equal to  $-34.3 \pm 0.1$  mV and  $-33.1 \pm 0.1$  mV, respectively (Figs. 3B and D). The average sizes of the AvAgNPs F24 and F40 were 100.6 and 100 nm, respectively. It could be concluded that the isoelectric point was below pH = 3. At pH > 7, the particles were fairly stable owing to electrostatic repulsion.

FTIR analysis of the *Achiella vermicularis* flower hot water extract exhibited a spectrum of different IR bands of hydroxyl ( $3200\text{--}3650$   $\text{cm}^{-1}$ ), alkanes ( $1340\text{--}1470$   $\text{cm}^{-1}$ ,  $2850\text{--}2970$   $\text{cm}^{-1}$ ), alkyne ( $2100\text{--}2260$   $\text{cm}^{-1}$ ), carbonyl ( $1690\text{--}1760$   $\text{cm}^{-1}$ ), C=C alkenes ( $1610\text{--}1680$   $\text{cm}^{-1}$ ), C=C aromatic ring ( $1500\text{--}1600$   $\text{cm}^{-1}$ ), aromatic amines ( $1300\text{--}1370$   $\text{cm}^{-1}$ ), amine–amide ( $1180\text{--}1360$   $\text{cm}^{-1}$ ), alcohol, carboxylic acid ( $1050\text{--}1300$   $\text{cm}^{-1}$ ), and aliphatic amines ( $1040\text{--}1053$   $\text{cm}^{-1}$ ). These functional groups have been previously reported to contain phenolic, terpenoid, and volatile compounds (Gogoit *et al.*, 2015; Yang *et al.*, 2013). Flower IR band types were obtained at  $3318$   $\text{cm}^{-1}$  (OH);  $1375$ ,  $1490$ ,  $2853$ , and  $2924$   $\text{cm}^{-1}$  (alkanes);  $1612$   $\text{cm}^{-1}$  (alkenes);  $1734$   $\text{cm}^{-1}$  (carbonyl);  $1022$   $\text{cm}^{-1}$  (aliphatic amines);  $1185$   $\text{cm}^{-1}$  and  $1310$   $\text{cm}^{-1}$  (amine–amide);  $1238$

$\text{cm}^{-1}$  (carboxylic acid); and  $1610$   $\text{cm}^{-1}$  (C=C alkenes). Similar IR band types for AvAgNPs (F24) were obtained at  $3277$   $\text{cm}^{-1}$  (OH);  $1369$ ,  $1452$ ,  $2853$ , and  $2924$   $\text{cm}^{-1}$  (alkanes);  $1522$   $\text{cm}^{-1}$  (aromatic ring);  $1633$   $\text{cm}^{-1}$  (alkenes);  $1742$   $\text{cm}^{-1}$  (carbonyl); and  $1090$   $\text{cm}^{-1}$  (carboxylic acid) (Fig. 4A). AvAgNPs (F40) demonstrated similar IR bands with AvAgNPs (F 24) (Fig. 4B). The bands identified in the plants demonstrated that these bands overlapped for the synthesized particles; the AvAgNPs bands coincided. The results showed that the NPs were synthesized by plant flower extracts combined with Ag.

X-ray diffraction analyses were carried out to confirm the crystalline structure of the synthesized AvAgNPs. According to the XRD spectrum of the synthesized AvAgNPs, four distinct diffraction peaks were determined at  $2\theta = 37.98^\circ$ ,  $44.0^\circ$ ,  $64.0^\circ$ , and  $77.34^\circ$ , while the lattice plane value was observed where the Bragg's reflections were indexed at 111, 200, 220, and 311 of the cubic Ag (Fig. 5). The resulting XRD spectrum clearly suggested that the AgNPs synthesized from *Achiella vermicularis* flower water extract were crystalline. The XRD patterns showed that the findings of the present study are consistent with those from earlier reports (Bar *et al.*, 2009; Saravanakumar *et al.*, 2015).

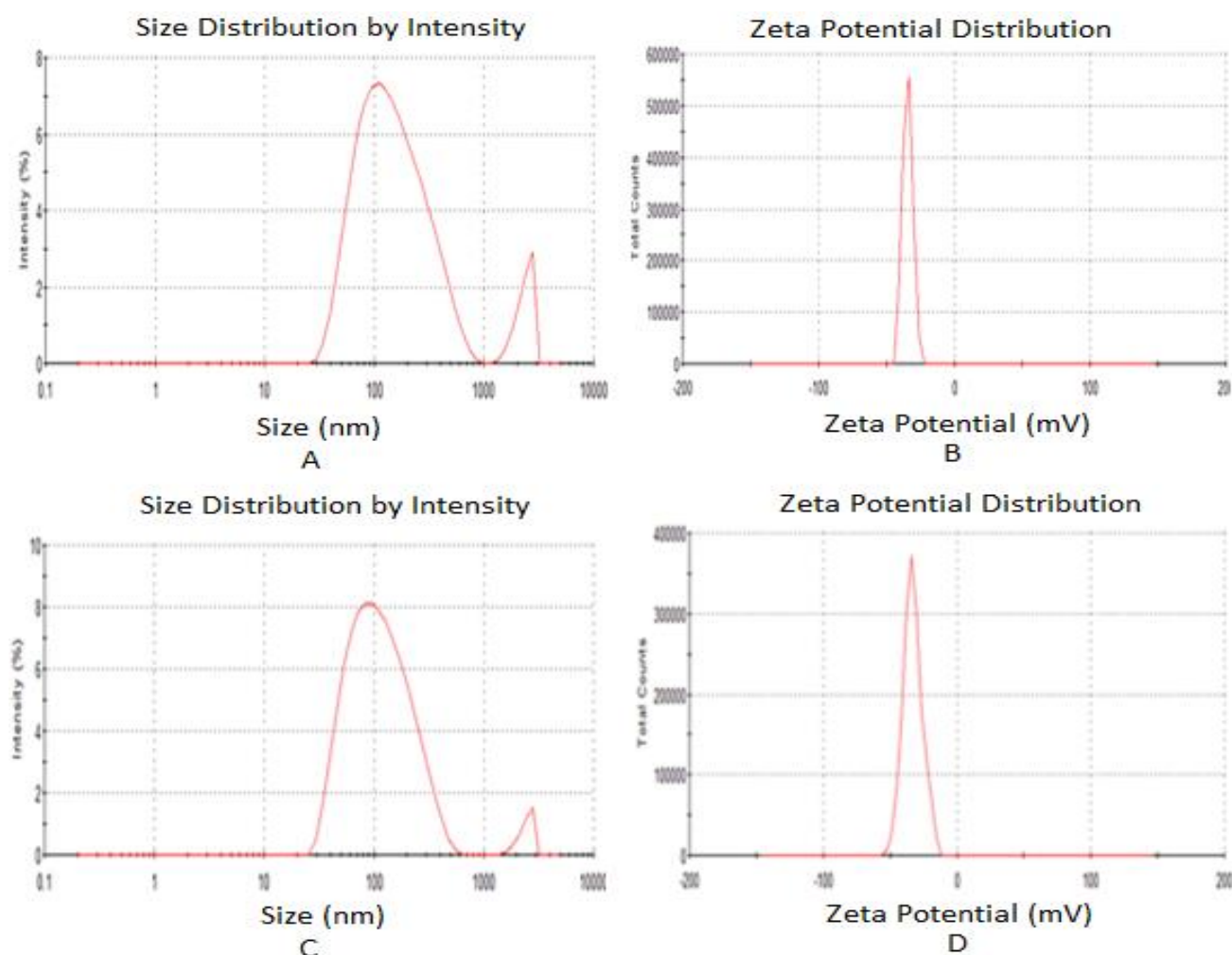


Fig. 3. Zeta potential and size distribution of synthesized silver nanoparticles (A) AvAgNPs (Flower 24) size distribution (B). AvAgNPs (Flower 24) Zeta potential (C) AvAgNPs (Flower 40) size distribution (B). AvAgNPs (Flower 40) Zeta potential.

The morphology of the AvAgNPs was examined by SEM (JEOL). Before the analysis, the samples were doped with 0.5% (w/v) phosphotungstic acid and placed on copper grids for observation. The NP sizes obtained with the micrograph showed similarities with the zeta measurements results. Aggregation was observed on the SEM micrographs (Fig. 6A, B)

**In vitro antioxidant activity:** It is generally known that phenolic substances exhibit anti-oxidant properties. The extracts and AvAgNPs were therefore used in the determination of total phenolic and flavonoid compounds. The total phenolic and flavonoid amounts are listed in Table 1. The phenolic content of the AvAgNPs flower was found to be approximately 1/40 of the flower extract, and notwithstanding, the anti-oxidant properties of NPs did not demonstrate differences when compared to pure plant extracts.

The free radical scavenging effect of AvAgNPs, extracts, and standards were determined by a DPPH assay. The DPPH scavenging activity is known to accept hydrogen or electrons. Thereby, the DPPH pink colour turns to yellow. The DPPH-scavenging activities are shown in Fig. 7. The DPPH activity of the NPs and extracts was evaluated by the phenolic compound.

According to this evaluation, the phenolic sources of the plant extract were higher than those of the NPs. The biosynthesized particle concentrations for 200  $\mu\text{g/ml}$  were found to be similar for all particle types, which was close to 50% of the inhibition values. These values were significantly higher compared to the standard anti-oxidants and extracts. The IC<sub>50</sub> of AvAgNPs F24 and F40, flower extracts, BHA, and ascorbic acid were found to be 197 and 200, 112.35, 384.61, and 370.41  $\mu\text{g/ml}$ , respectively, showing the dominant potency of pure plant extracts, followed by AvAgNPs F 24. The study results demonstrated that AvAgNPs had more effective DPPH scavenging inhibition that was higher than those of the standard anti-oxidant BHA and ascorbic acid. The findings shown in Fig. 7 indicate that the obtained results were similar to those of previous studies (Nakkala *et al.*, 2015; Nakkala *et al.*, 2014; Shanmugam *et al.*, 2015).

The metal chelating activities of the AvAgNPs F24 and F40, the flower extract, and the EDTA were found to be 71.43% and 71.62%, 85.29%, and 97.66% for concentrations of 200  $\mu\text{g/ml}$ , respectively. The metal chelating activities of the AvAgNPs and the extracts are shown as a bar chart in Fig. 8. The results demonstrated that AvAgNPs and extract had similar reduction powers and activities (Kanipandian *et al.*, 2014).

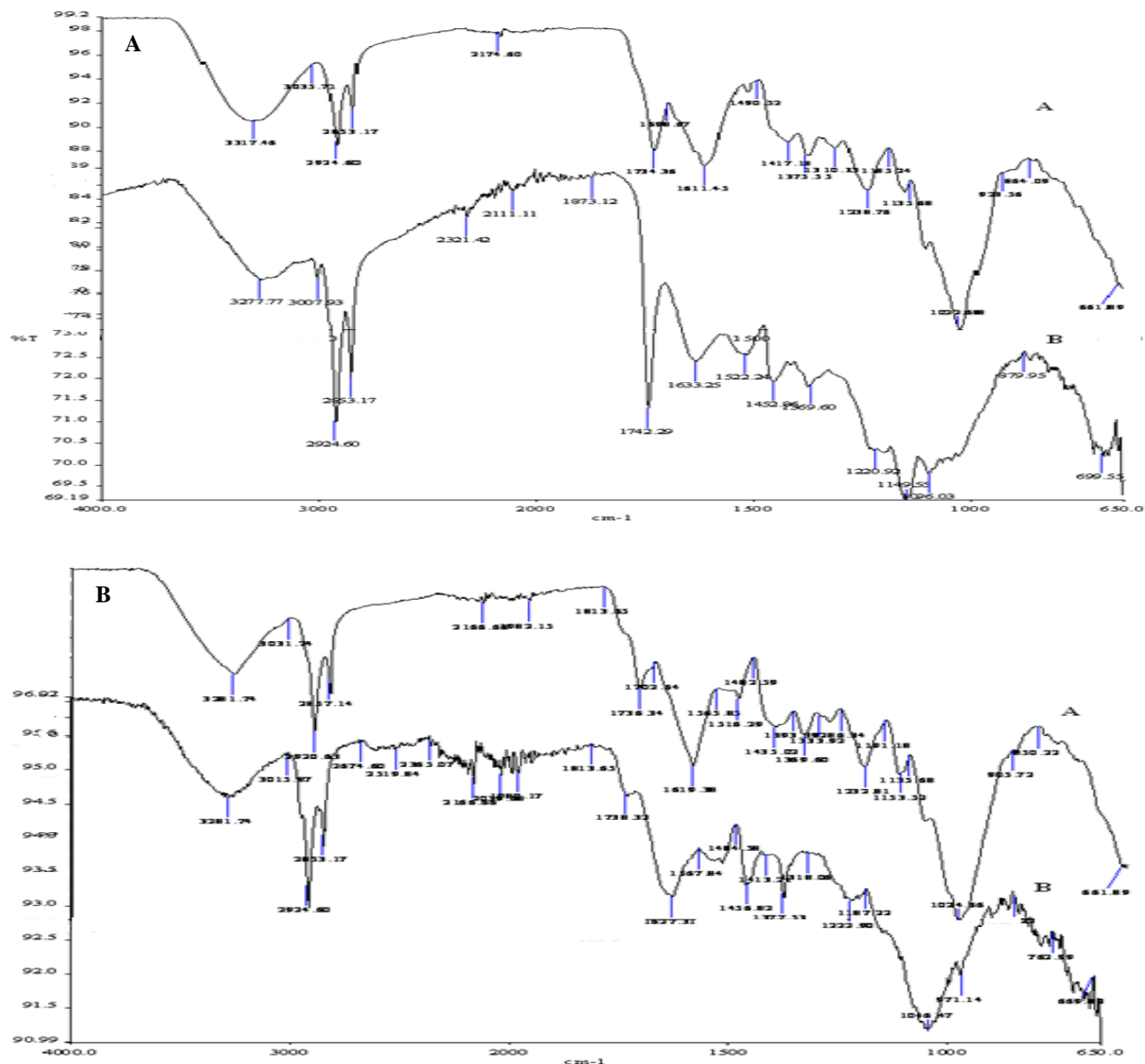


Fig. 4. FTIR spectra of synthesized silver nanoparticles (A) AvAgNPs Flower 24 (A. Extract B. AvAgNPs (Flower 24)) (B). AvAgNPs Flower 40 (A. Extract B. AvAgNPs (Flower 40))

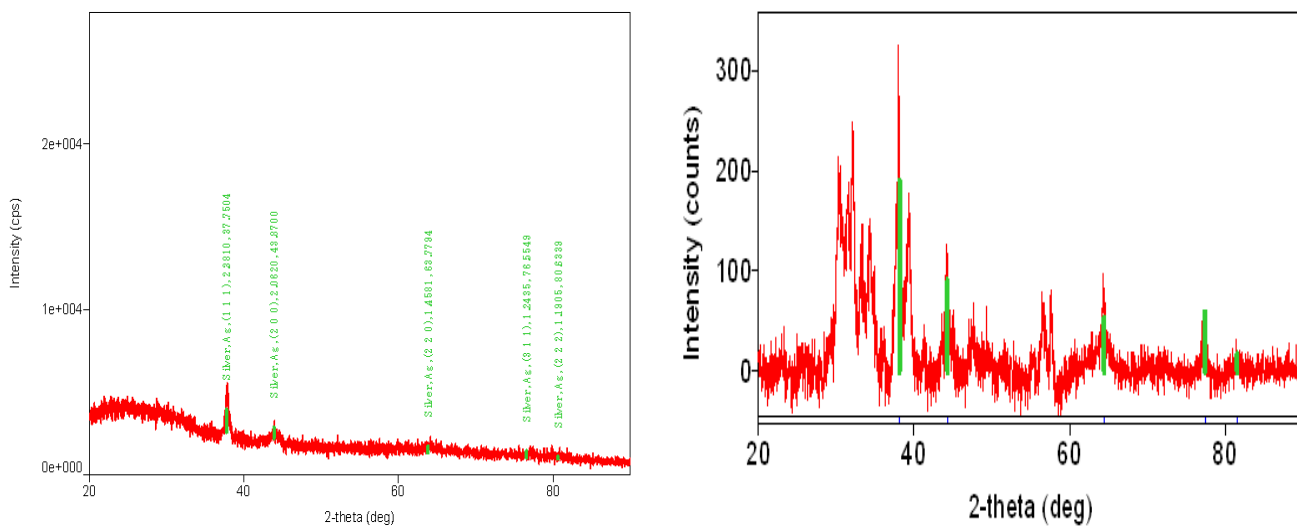


Fig. 5. XRD of synthesized silver nanoparticles (A) AvAgNPs (Flower 24) (B). AvAgNPs(Flower 40).

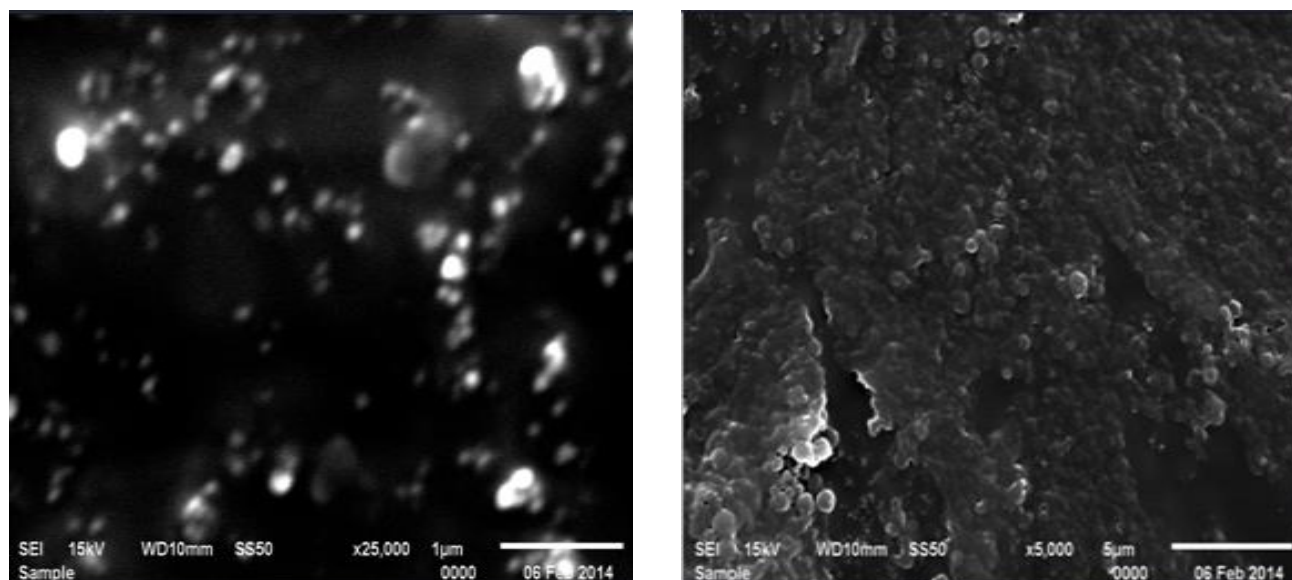


Fig. 6. SEM of synthesized silver nanoparticles (A) AvAgNPs (Flower 24) (B). AvAgNPs (Flower 40).

**Table 1. Total phenolic, phenolic acid and flavonoid contents of nanoparticles and extract.**

Product	Total phenolic content ( $\mu\text{g gallic acid/g d.w.}$ )	Total phenolic acid content ( $\mu\text{g sinapic acid/g d.w.}$ )	Total flavonoid content ( $\mu\text{g catechin/g d.w.}$ )
Flower 24	68.9 $\pm$ 2.6	388.9 $\pm$ 212.5	571.3 $\pm$ 335.9
Flower 40	25.9 $\pm$ 6.6	187.5 $\pm$ 70.7	195.3 $\pm$ 39.3
Flower extract	2313.3 $\pm$ 75.3	116612.5 $\pm$ 6293.3	2228.5 $\pm$ 20.6

Values are expressed in mean  $\pm$  SEM (n =3)

**Table 2. Antimicrobial effect of nanoparticles (Table 2).**

Microrganism	AvAgPNs F24	AvAgPNs F40	(+) Control	(-) Control	Flower extract	AgNO <sub>3</sub>	Flower extract +AgNO <sub>3</sub>
<i>E. coli</i> (ATCC 2592)	7,9 $\pm$ 0.1	8,9 $\pm$ 0.1	17,7 $\pm$ 0.1	6	6	7,0 $\pm$ 0.1	8,7 $\pm$ 0.1
<i>L. monocytogenes</i> (NCTC 5348)	9,1 $\pm$ 0.1	6,8 $\pm$ 0.1	10,9 $\pm$ 0.1	6	6	8,9 $\pm$ 0.1	8,3 $\pm$ 0.1
<i>S. aureus</i> (ATCC 6538P)	9,3 $\pm$ 0.1	6,7 $\pm$ 0.1	12,9 $\pm$ 0.1	6	6	8,2 $\pm$ 0.1	8,5 $\pm$ 0.1
<i>S. cerevisiae</i> ATCC 76521	7,4 $\pm$ 0.1	6,0 $\pm$ 0.1	14,8 $\pm$ 0.1	6	6	7,2 $\pm$ 0.1	7,4 $\pm$ 0.1

Note: All analyses were repeated 3 times and found within \* p<0.05 confidence interval. Those with an inhibition zone of under 1 mm did not demonstrate antimicrobial activity. Low antimicrobial activity indicates antimicrobial activity as inhibition zone 2–3 mm. Average antimicrobial activity inhibition zone is determined as 4–5 mm. High antimicrobial activity inhibition zone is identified as 6–9 mm and strong antimicrobial activity inhibition zone is expressed as >9 mm. Streptomycin (Str) discs were used as positive control. DMSO (Merck) was used as negative control. (\*) Figures indicate the inhibition zone diameters. Each disc had a 6 mm diameter and each disc was saturated with 40  $\mu\text{l}$  sample (1 mg/ml). Values are expressed in mean  $\pm$  SEM (n =3)

The H<sub>2</sub>O<sub>2</sub> radical scavenging effect was investigated to determine the anti-oxidant potential of the NPs. The hydrogen radical source in biological systems is hydrogen peroxide. This radical can cause serious damage to the cells and cell membranes. The hydrogen peroxide scavenging activities of AvAgNPs and extracts are presented in Fig. 9. The results indicated that the AvAgNPs were fairly potent in scavenging hydroxyl radicals. The AvAgNPs were more effective than BHA, ascorbic acid, and the flower extract. The metal chelating activities of the AvAgNPs F24 and F40, the flower extract, BHA, and ascorbic acid were found to be 77.53% and 87.42%, 19.04%, 25.43%, and 53.62% for concentrations of 200  $\mu\text{g/ml}$ , respectively.

**Antibacterial activity:** The AvAgNPs, AgNO<sub>3</sub>, AgNO<sub>3</sub>-*Achillea vermicularis* extracts, *Achillea vermicularis* extracts, and antibiotic streptomycin were tested for the anti-microbial activity. The biosynthesized Ag NPs were analysed against *Saccharomyces cerevisiae* and various pathogenic organisms, such as *Staphylococcus aureus*, *Listeria monocytogenes*, and *Escherichia coli* using the disc diffusion method (Table 2). The microbial growth of bacteria and yeast was influenced in 1 mg/ml AvAgNP concentration and AvAgPNs F24 AvAgPNs F40, (+) Control (Streptomycin (Str)), (-) Control (DMSO), Flower Extract, AgNO<sub>3</sub> and Flower Extract+AgNO<sub>3</sub>.

**Effects of AvAgNPs on PC-3 cell proliferation:** The anti-cell proliferative effect of the AvAgNPs and extracts were assessed using a WST-1 assay. The cytotoxic effects of the AvAgNPs and extracts on PC-3 cells were investigated. The cells were treated with various concentrations of AvAgNPs, ranging from 15,625 mg/l to 250 mg/l over 48 h, and the percentage inhibition results of cell proliferation are shown in Fig. 10. All extract concentrations had cytotoxic effects on PC-3 cells. All AvAgNPs (F24 and F40) significantly decreased the PC-3 cell proliferation at concentrations of 250  $\mu\text{g}/\text{mL}$ , compared to the control cells ( $p < 0.001$ ) (Figs. 10A and B). Previous studies that focused on *Achillea vermicularis* evaluated the cytotoxic activities against MCF-7 and A-549 cell lines. The study results determined *Achillea vermicularis* IC50 values below 100  $\mu\text{g}/\text{mL}$  (Hamzeloo-Moghadam *et al.*; Naghibi *et al.*, 2015).

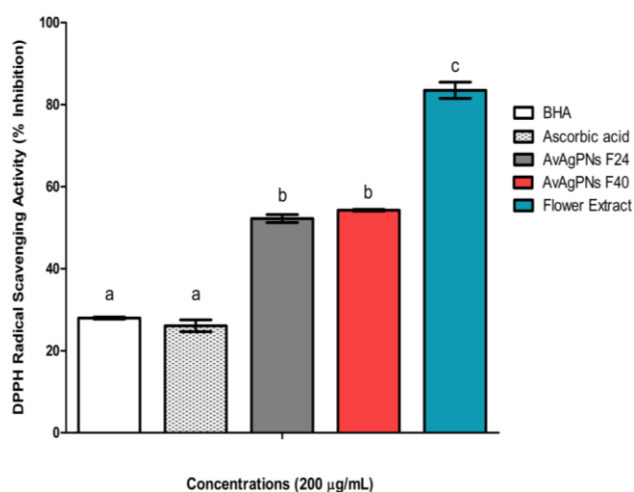


Fig. 7. DPPH reduction activity of synthesized silver nanoparticles, extract and standards. (a-c: Values followed by different letters are significantly different at  $p < 0.05$  as determined by one-way ANOVA (Analysis of variance) by Tukey's multiple comparison test.)

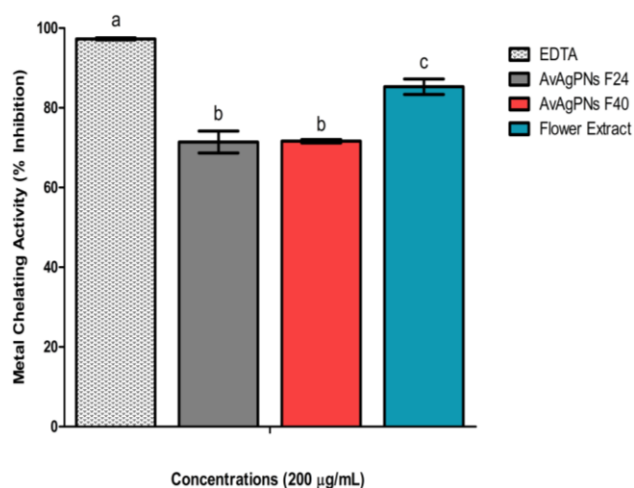


Fig. 8. Metal chelating activity of synthesized silver nanoparticles, extract and EDTA. (a-d: Values followed by different letters are significantly different at  $p < 0.05$  as determined by one-way ANOVA (Analysis of variance) by Tukey's multiple comparison test.)

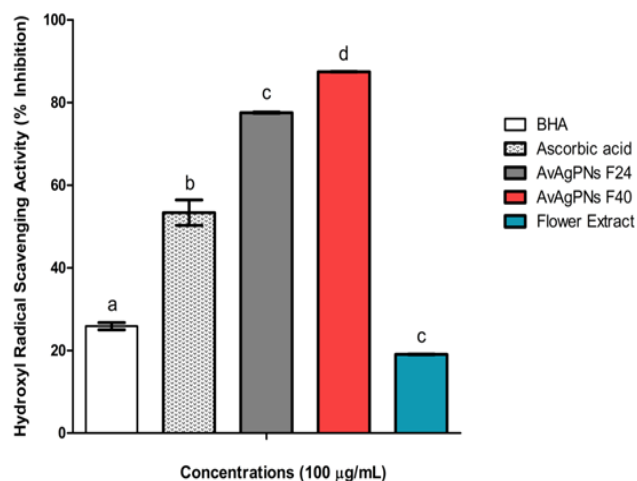


Fig. 9. Hydroxyl radical scavenging activity of synthesized silver nanoparticles, extract and standards. (a-d: Values followed by different letters are significantly different at  $p < 0.05$  as determined by one-way ANOVA (Analysis of variance) by Tukey's multiple comparison test.)

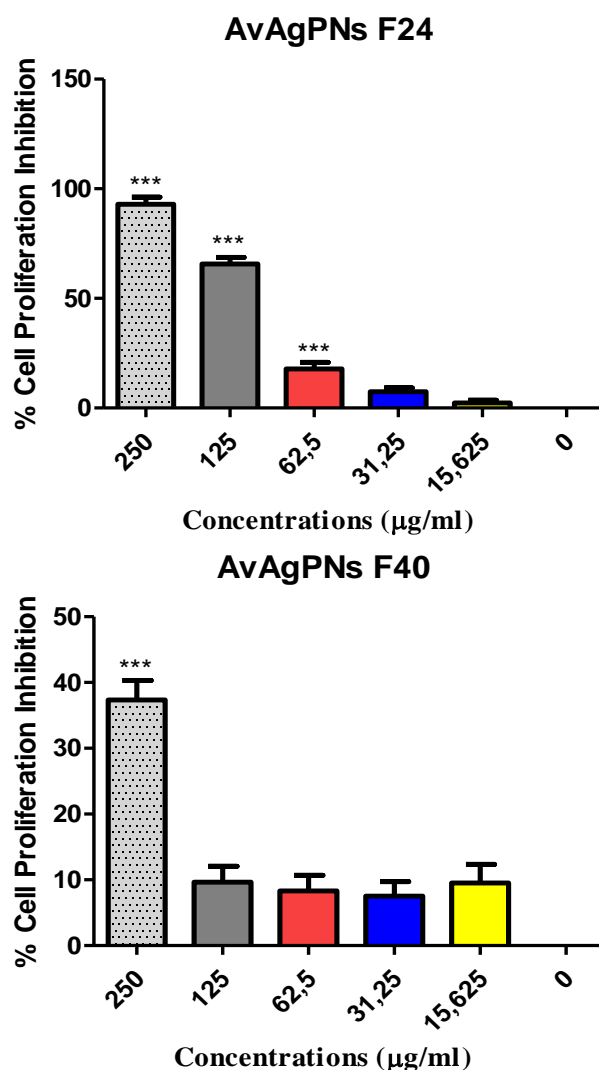


Fig. 10. Statistical analysis was performed with GraphPad Prism 5.01 software and comparable data sets were evaluated by the one-way ANOVA Newman-Keuls Post-Hoc Test;  $p < 0.05$  was considered significant. Anticancer activity of AvAgNPs in PC-3 cell line A) AvAgNPs Flower 24 B) AvAgNPs Flower 40. (\*\*\*) $p < 0.0001$ ; 0  $\mu\text{g}/\text{mL}$  vs 250  $\mu\text{g}/\text{mL}$ , 125  $\mu\text{g}/\text{mL}$ , 62.5  $\mu\text{g}/\text{mL}$ .

## Conclusion

Green syntheses of NPs yield metal NPs that can be employed in several industrial and medical fields. Researchers are involved in developing methods and sources that are cost-effective for extracting and incorporating NPs for their respective uses. However, these NPs raise environmental and health concerns due to their harmful properties. Ag NPs are largely used commercially, and hence, the environment and individuals are more exposed to their adverse effects. Ag NPs are also applicable to medicine, food, and cosmetic products for their anti-microbial, anti-oxidant, and anti-cancer properties.

In the present study, Ag NPs were obtained within a short time by using a biological method (green synthesis). The particles that were obtained were polydisperse and spherical. The NPs' formation was obtained using surface plasmon resonance with a combination of plants' active ingredients with Ag. The formation of the NPs was characterised using UV-vis spectroscopy, AFM, XRD, zeta sizer, FT-IR, SEM, and FT-IR methods. These characterisation studies demonstrated that carbonyl and amino groups on the amino acid sequence bound tightly to Ag. The zeta potential results indicated that NP formation inhibited the aggregation of NPs. The AFM results supported these findings that NPs were placed properly. Anti-microbial studies indicated that Ag NPs synthesised with low concentrations of the extract showed higher activities among themselves. In addition, the anti-proliferation activities of the NPs greatly impacted the PC-3 prostate cancer cell line.

## References

- Abdel-Aziz, M.S., M.S. Shaheen, A.A. El-Nekeety and M.A. Abdel-Wahhab. 2014. Antioxidant and antibacterial activity of silver nanoparticles biosynthesized using *Chenopodium murale* leaf extract. *J. Saudi Chem. Soc.*, 18(4): 356-363.
- Abou El-Nour, K.M.M., A. Eftaiha, A. Al-Warthan and R.A.A. Ammar. 2010. Synthesis and applications of silver nanoparticles. *Arabian Journal of Chemistry*, 3(3): 135-140.
- AlSalhi, M.M.S. and M.K.J. Siddiqui. 2010. Silver nanoparticle applications and human health. *Clin. Chim. Acta*, 411(23-24): 1841-1848.
- Awwad, A., N. Salem and A. Abdeen. 2013. Green synthesis of silver nanoparticles using *Carob* leaf extract and its antibacterial activity. *Int. J. of Ind. Chem.*, 4(1): 29.
- Bar, H., D.K. Bhui, G.P. Sahoo, P. Sarkar, S. Pyne and A. Misra. 2009. Green synthesis of silver nanoparticles using seed extract of *Jatropha curcas*. *Colloids Surf., A*, 348(1-3): 212-216.
- Barani, H., M. Montazer, N. Samadi and T. Toliyat. 2011. Nano silver entrapped in phospholipids membrane: Synthesis, characteristics and antibacterial kinetics. *Mol. Membr. Biol.*, 28(4): 206-215.
- Barros, L., M.-J. Ferreira, B. Queirós, I.C.F.R. Ferreira and P. Baptista. 2007. Total phenols, ascorbic acid,  $\beta$ -carotene and lycopene in portuguese wild edible mushrooms and their antioxidant activities. *Food Chem.*, 103(2): 413-419.
- Baytop, T. 1999. Türkiye'de bitkiler ile tedavi. (second ed.) Edn., İstanbul Nobel Tıp Kitabevi.
- Chen, X. and H.J. Schluesener. 2008. Nanosilver: A nanoparticle in medical application. *Toxicol. Lett.*, 176(1): 1-12.
- Collart, D.M.S., L. Robinson, B. Kepner and E.A. Mintz. 2006. Efficacy of oligodynamic metals in the control of bacteria growth in humidifier water tanks and mist droplets. *J. Water Health.*, 4(2): 149-156.
- Dinis, T.C.P., V.M.C. Madeira and L.M. ve Almeida, L. M., 1994. Action of phenolic derivatives (acetoaminophen, salicylate, and 5-aminosalicylate) as inhibitors of membrane lipid peroxidation and peroxy radicals scavengers. *Arch. Biochem. Biophys.*, 315: 161-169.
- Gamez-Meza, N., J.A. Noriega-Rodriguez, L.A. Medina-Juarez, J. Ortega-Garcia, R. Cazarez-Casanova and O. Angulo-Guerrero, 1999. Antioxidant activity in soybean oil of extracts from thompson grape bagasse. *J. Am. Oil Chem. Soc.*, 76(12): 1445-1447.
- Gogoi, N., P.J. Babu, C. Mahanta and U. Bora, 2015. Green synthesis and characterization of silver nanoparticles using alcoholic flower extract of *Nyctanthes arbortristis* and *In vitro* investigation of their antibacterial and cytotoxic activities. *Mater. Sci. Eng., C* 46: 463-469.
- Gopinath, P., S.K. Gogoi, A. Chattopadhyay and S.S. Ghosh, 2008. Implications of silver nanoparticle induced cell apoptosis for *In vitro* gene therapy. *Nanotechnology*, 19(7): 075104.
- Hamzeloo-Moghadam, M., A. Khalaj, M. Malekmohammadi and M. Mosaddegh, 2015. *Achillea vermicularis* a medicinal plant from iranian traditional medicine induces apoptosis in mcf-7 cells. *Res. J. Pharmacogn.*, 2(1): 1-5.
- Harris, A.T., R. Bali, 2008. On the formation and extent of uptake of silver nanoparticles by live plants. *J. Nanopart. Res.*, 10(4): 691-695.
- Hatano, T., H. Kagawa, T. Yasuhara and T. Okuda, 1988. 2 new flavonoids and other constituents in licorice root - their relative astringency and radical scavenging effects. *Chem. Pharm. Bull.*, 36(6): 2090-2097.
- Jayaseelan, C., R. Ramkumar, A.A. Rahuman and P. Perumal, 2013. Green synthesis of gold nanoparticles using seed aqueous extract of *Abelmoschus esculentus* and its antifungal activity. *Ind. Crop. Prod.*, 45: 423-429.
- Kanipandian, N., S. Kannan, R. Ramesh, P. Subramanian and R. Thirumurugan, 2014. Characterization, antioxidant and cytotoxicity evaluation of green synthesized silver nanoparticles using *Cleistanthus collinus* extract as surface modifier. *Mater. Res. Bull.*; 49: 494-502.
- Kaya, B., Y. Menemen and F.Z. Saltan. 2012. Flavonoids in the endemic species of *Alchemilla* L., (section *Alchemilla* L. subsection *calycanthum* Rothm. Ser. *Elatae* Rothm.) from North-East Black Sea Region in Turkey. *Pak. J. Bot.*, 44(2): 595-597.
- Kelly, K.L., E. Coronado, L.L. Zhao and G.C. Schatz, 2003. The optical properties of metal nanoparticles: The influence of size, shape, and dielectric environment. *J. Phys. Chem. B*, 107(3): 668-677.
- Kim, T.H., M. Kim, H.S. Park, U.S. Shin, M.S. Gong and H.W. Kim, 2012. Size-dependent cellular toxicity of silver nanoparticles. *J. Biomed. Mater. Res. A*, 100(4): 1033-1043.
- Liu, N., L.X. Li, G.H. Cao and R. Lee, 2010. Silver-embedded zeolite thin film-based fiber optic sensor for in situ, real-time monitoring  $Hg^{2+}$  ions in aqueous media with high sensitivity and selectivity. *J. Mater. Chem.*, 20(41): 9029-9031.
- Makarov, V.V., A.J. Love, O.V. Sinitsyna, S.S. Makarova, I.V. Yaminsky, M.E. Taliansky and N.O. Kalinina, 2014. "Green" nanotechnologies: Synthesis of metal nanoparticles using plants. *Acta Naturae*, 6(1): 35-44.
- Manceau, A., K.L. Nagy, M.A. Marcus, M. Lanson, N. Geoffroy, T. Jacquet and T. Kirpichtchikova, 2008. Formation of metallic copper nanoparticles at the soil-root interface. *Environ. Sci. Technol.*, 42(5): 1766-1772.

- Martínez-Gutierrez, F., Thi, E. P., Silverman, J. M., de Oliveira, C. C., Svensson, S. L., Hoek, A. V., Bach, H. , 2012. Antibacterial activity, inflammatory response, coagulation and cytotoxicity effects of silver nanoparticles. *Nanomedicine: NBM*, 8(3): 328-336.
- Mohanty, S., S. Mishra, P. Jena, B. Jacob, B. Sarkar and A. Sonawane, 2012. An investigation on the antibacterial, cytotoxic, and antibiofilm efficacy of starch-stabilized silver nanoparticles. *Nanomedicine*, 8(6): 916-924.
- Naghbi, F., A. Khalaj, M. Mosaddegh, M. Malekmohamadi and M. Hamzelo-Moghadam, 2014. Cytotoxic activity evaluation of some medicinal plants, selected from iranian traditional medicine pharmacopoeia to treat cancer and related disorders. *J. Ethnopharmacol.*, 155(1): 230-239.
- Nakkala, J.R., E. Bhagat, K. Suchiang and S.R. Sadras, 2015. Comparative study of antioxidant and catalytic activity of silver and gold nanoparticles synthesized from *Costus pictus* leaf extract. *J. Mater. Sci. Technol.*, 31(10): 986-994.
- Nakkala, J.R., R. Mata, A.K. Gupta and S.R. Sadras, 2014. Biological activities of green silver nanoparticles synthesized with *Acorous calamus* rhizome extract. *Eur. J. Med. Chem.*, 85: 784-794.
- Oves, M., M.S. Khan, A. Zaidi, A.S. Ahmed, F. Ahmed, E. Ahmad, A. Sherwani, M. Owais and A. Azam, 2013. Antibacterial and cytotoxic efficacy of extracellular silver nanoparticles biofabricated from chromium reducing novel os4 strain of *Stenotrophomonas maltophilia*. *PLoS One*, 8(3): e59140.
- Rai, M., A. Yadav and A. Gade, 2009. Silver nanoparticles as a new generation of antimicrobials. *Biotechnol. Adv.*, 27(1): 76-83.
- Roh, J.Y., S.J. Sim, J. Yi, K. Park, K.H. Chung, D.Y. Ryu and J. Choi, 2009. Ecotoxicity of silver nanoparticles on the soil nematode *Caenorhabditis elegans* using functional ecotoxicogenomics. *Environ. Sci. Technol.*, 43(10): 3933-3940.
- Ruch, R.J., S.J. Cheng and J.E. Klaunig, 1989. Prevention of cytotoxicity and inhibition of intercellular communication by antioxidant catechins isolated from chinese green tea. *Carcinogenesis*, 10(6): 1003-1008.
- Saravanakumar, A., M. Ganesh, J. Jayaprakash and H.T. Jang, 2015. Biosynthesis of silver nanoparticles using cassia tora leaf extract and its antioxidant and antibacterial activities. *J. Ind. Eng. Chem.*, 28: 277-281.
- Shanmugam, C., G. Sivasubramanian, B. Parthasarathi, K. Baskaran, R. Balachander and V.R. Parameswaran, 2015. Antimicrobial, free radical scavenging activities and catalytic oxidation of benzyl alcohol by nano-silver synthesized from the leaf extract of *Aristolochia indica* L.: a promenade towards sustainability. *Appl. Nanosci.* 6(5):711-713.
- Sintubin, L., De Windt, W., Dick, J., Mast, J., van der Ha, D., Verstraete, W., 2009. Lactic acid bacteria as reducing and capping agent for the fast and efficient production of silver nanoparticles. *Appl. Microbiol. Biotechnol.*, 84: 741-749.
- Thakkar, K.N., S.S. Mhatre and R.Y. Parikh, 2010. Biological synthesis of metallic nanoparticles. *Nanomedicine*, 6(2): 257-262.
- Veerasingam, R., T. Xin, S. Gunasagaran, T. Xiang, E. Yang, N. Jeyakumar and S. Dhanaraj, 2011. Biosynthesis of silver nanoparticles using *Mangosteen* leaf extract and evaluation of their antimicrobial activities. *J. Saudi Chem. Soc.* 15: 113 - 120.
- Yang, N. and W.-H. Li, 2013. *Mango peel* extract mediated novel route for synthesis of silver nanoparticles and antibacterial application of silver nanoparticles loaded onto non-woven fabrics. *Ind. Crop. Prod.*, 48: 81-88.
- Zhang, W., Y. Yao, N. Sullivan and Y.S. Chen, 2011. Modeling the primary size effects of citrate-coated silver nanoparticles on their ion release kinetics. *Environ. Sci. Technol.*, 45(10): 4422-4428.
- Zook, J.M., R.I. MacCuspie, L.E. Locascio, M.D. Halter and J.T. Elliott, 2011. Stable nanoparticle aggregates/agglomerates of different sizes and the effect of their size on hemolytic cytotoxicity. *Nanotoxicology*, 5(4): 517

(Received for publication 16 September 2017)